Food and Bioprocess Technology
https://doi.org/10.1007/s11947-024-03359-3

RESEARCH

Optimization of Synthesis Reaction Parameters of AgNPs Derived from *Laser trilobum* Plant for Foodborne Pathogens

Ali Soyucok[1] · **Burcu Kabak**[2] · **Bekir Tosun**[3]

Received: 1 February 2024 / Accepted: 1 March 2024

Abstract

In this study, the antimicrobial activity of silver nanoparticles (AgNPs L_{21}, AgNPs L_{22}) produced using aqueous extracts of the *Laser trilobum* harvested in 2021 and 2022 was optimized. The experimental design and optimization of antimicrobial activity were performed using the response surface method (RSM). Using RSM, independent variables, such as silver concentration, extraction time, and synthesis temperature, were optimized as a result of the inhibition zone diameter against *Staphylococcus aureus*, *Escherichia coli*, *Salmonella* Typhimurium, and *Listeria monocytogenes*. Based on the optimization results, the extraction time, silver concentration, and temperature for AgNP L_{21} and L_{22} synthesis were determined to be 60 min, 5 mM, and 25 °C, respectively. When the XRD and TEM results of the nanoparticles synthesized under optimal conditions were evaluated, it was determined that the AgNPs were spherical in shape and had an average size of 30 ± 12 nm. Our study revealed that the year of harvest is unimportant for nanoparticles synthesized from *L. trilobum*, using a cheap and simple method that does not require toxic substances. Owing to the antimicrobial activity of nanoparticles produced under optimal conditions, it is possible to biocontrol and prevent contamination by these bacteria in food science and industry.

Keywords AgNPs · Foodborne pathogens · Green synthesis · *Laser trilobum* · Process optimization · Response surface method

Introduction

Microbial contamination is one of the most serious food spoilage problems. Microbial deterioration and/or foodborne outbreaks occur as a result of microbial contamination. The presence of bacteria causing microbial contamination adversely affects consumer preferences and health (Özer & Kılıç, 2021). Food additives are used to overcome economic loss and food safety problems. In particular, the toxicity and carcinogenic effects of synthetic food additives are doubtful. Moreover, natural additives have been an attractive alternative for consumers and the food industry for healthy food and serve as alternatives to synthetic additives (Soyuçok et al., 2019). These natural additives are bioactive compounds originating from plants, beneficial microorganisms, and animals (Mahmud & Khan, 2018).

Plants contain volatile and aromatic compounds, which are effective against microbial spoilage. It reduces the possibility of foodborne epidemics in humans due to the bactericidal and bacteriostatic effects of plant extracts against microorganisms (Batiha et al., 2021). Most plant-derived antimicrobial compounds are generally recognized as safe (GRAS) (Mahmud et al., 2023). Biomolecules—obtained from plants using various extraction methods—have been reported to possess antimicrobial properties against foodborne pathogens such as *Bacillus cereus*, *Escherichia coli*, *Listeria monocytogenes*, *Staphylococcus aureus*, and *Salmonella* (Batiha et al., 2021).

✉ Burcu Kabak
burcukabak@hotmail.com

Ali Soyucok
alisoyucok@gmail.com

Bekir Tosun
btosun@mehmetakif.edu.tr

[1] Department of Food Processing, Burdur Food Agriculture and Livestock Vocational School, Burdur Mehmet Akif Ersoy University, 15100 Burdur, Türkiye

[2] Chemistry Department, Faculty of Arts and Science, Burdur Mehmet Akif Ersoy University, 15100 Burdur, Turkey

[3] Agriculture, Livestock and Food Research and Application Center, Burdur Mehmet Akif Ersoy University, 15100 Burdur, Türkiye

Published online: 04 March 2024

Nanotechnology is a highly promising area of research in nanoscience and technology, as it encompasses interdisciplinary interactions with various scientific disciplines such as physics, chemistry, food, biology, and materials science (Mohanta et al., 2020; Trak & Arslan, 2022). There has been a significant surge in the interest in nanoscale materials over the past decade. Nanoparticles (NPs) have a significant impact on many applications, including magnetic (Ma et al., 2022), optoelectronics (Chen et al., 2016), functional biology (Rashidian et al., 2023), photocatalysis (Sunil Kumar et al., 2022), drug delivery (Al Dine et al., 2017), and antibacterial (Maciel et al., 2020; Mohanta et al., 2018) studies because of their new or improved characteristics, such as sizes ranging from 1 to 100 nm, different forms, and specific structures (Behravan et al., 2019; Hashemi et al., 2022; Jadhav et al., 2015; Khan et al., 2023).

Metallic nanoparticle synthesis can be classified into two distinct methodologies: top-down and bottom-up. In top-down procedures, the size of bulk materials is decreased to a range, 10–100 nm, whereas in the bottom-up approach, the prepared materials are formed into larger nanostructures by means of atom or molecule linkage (Hoseinpour & Ghaemi, 2018; Ozkan et al., 2023; Shaikh et al., 2019).

Several physical and chemical processes employed for the synthesis of nanoparticles are characterized by high costs and the utilization of toxic and hazardous compounds, which pose potential environmental and biological risks owing to their structural properties. Therefore, it is important to find environmentally and economically compatible alternative methods for the preparation of nanoparticles in order to eliminate these disadvantages (Mahapatra et al., 2022; Trak & Arslan, 2021).

The green synthesis method is considered more appropriate than physical and chemical approaches because of its environmentally benign nature, cost-effectiveness, and adaptability for large-scale synthesis (Chandhru et al., 2019). Three different sources of bacteria, fungi, and plant extracts were used for the production of nanoparticles using the green synthesis method. Among these three main sources, the use of plant extracts is advantageous because of their easy accessibility to synthesize nanoparticles, their safety, and, in most cases, their non-toxic nature, which can help reduce metal ions (Agarwal et al., 2016; Tripathi et al., 2020). Plant ingredients include a range of chemical compounds, such as terpenoids, flavonoids, ketones, aldehydes, amides, and carboxylic acids. These compounds play a direct role in the reduction of ions and subsequent formation of metallic nanoparticles (Behravan et al., 2019).

The Apiaceae family is home to many aromatic plants that are used in food (Hajji et al., 2021), cosmetics (Thiviya et al., 2021), and healing (Thiviya et al., 2022). The seeds, flowers, stems, leaves, and roots of taxa in the Apiaceae family are rich sources of volatile oils (Cianfaglione et al., 2017; Tel-Çayan & Duru, 2019). The perennial species *Laser trilobum* (L.) Borkh, a member of the Apiaceae family, typically reaches a height of 50–120 cm. It is characterized by its hairless stems and white flowers. Seed production occurs from July to August. The species typically grows beneath pine forests, and its mature fruits are different locally used as spices under the Turkish names "kefe kimyonu, dağ kimyonu, sıra" (Baytop, 1999). In a previous study, the efficacy of this particular spice and its volatile oil as inhibitors of various bacteria in culture conditions was investigated. The results indicated that the pulverized fruit had a more pronounced inhibitory effect compared to the volatile oil (Facciola, 1990; Kivanc & Akgül, 1991).

Response surface methodology (RSM) accurately determines the relationship between independent parameters and system responses by estimating the variation trend (He et al., 2022; Shabaani et al., 2020). The response surface method (RSM) has many advantages, such as efficient investigation of factors, reduction of experimental runs, determination of optimal conditions, quantitative evaluation of factors, response estimation, robustness testing, information on synergistic effects, time and resource saving, and process understanding (Abdi et al., 2022; Ofgea et al., 2022). To the best of our knowledge, the application of RSM to study the effects of important parameters (metal concentration, extraction time, synthesis temperature, etc.) of the green synthesis method on the antimicrobial activity of AgNPs has not yet been reported. In summary, this innovative work explored the optimization of operating parameters using RSM for the most efficient antimicrobial activity of AgNPs. AgNPs were synthesized in this study using *L. trilobum* plant extracts obtained over two different harvest years. Thus, the possible effects of plants harvested in different years on the physicochemical and antimicrobial effects of AgNPs were also investigated. AgNPs synthesized under optimum conditions determined by RSM were characterized using UV–Vis spectrometry, Fourier transform infrared spectroscopy (FTIR), X-ray diffraction (XRD), and transmission electron microscopy (TEM). The MIC and MBC values of the AgNPs were investigated against *Staphylococcus aureus*, *Escherichia coli*, *Salmonella* Typhimurium, and *Listeria monocytogenes*.

Materials and Methods

Chemical and Reagents

Silver nitrate ($AgNO_3$) was purchased from ISOLAB (Germany) and was used for the synthesis of AgNPs. Tryptic Soy Agar (TSA, Merck M105458, Germany), Mueller–Hinton II Broth (MHB, Merck M110293, Germany), Mueller–Hinton Agar (Merck 103,872, Germany), NaCl (Merck

106,404.1000, Germany), and 96-well plate (Corning Costar 3599, F-bottom) were used in this study.

Bacterial Strains and Plant

The pathogenic strains used in the antimicrobial studies included methicillin-resistant *Staphylococcus aureus* ATCC 43300, *Salmonella* Typhimurium ATCC 14028, *Escherichia coli* ATCC 25922, and *Listeria monocytogenes* ATCC 19115, obtained from Burdur Mehmet Akif Ersoy University, Faculty of Veterinary Medicine, Department of Food Hygiene and Technology Laboratory. Fully mature *L. trilobum* fruits were used as plant material.

Preparation of Plant Materials

The first fruits of *L. trilobum* were collected from their natural habitats in Isparta, Barla Mountain, Turkey, in 2017. Faculty of Agriculture, Isparta University of Applied Sciences (ISUBU), which is in the central district of Isparta (37° 45′ N, 30° 33′ E 1035 m), was chosen as the experimental area for the studies conducted. Seeds of the species were sown with four seeds in each hole, containing a 3:1 perlite/peat mixture. Selected seeds were sown into violas during the early autumn of 2017, followed by transplantation of seedlings in spring 2018, which were harvested upon maturity in 2019. The species continues to provide fruits between 2020 and 2022, which were also harvested. In this study, mature *L. trilobum* fruits were collected in July 2021 and 2022. The average temperature was similar in 2021 and 2022, when the fruits were collected. The total precipitation is 468.8 mm in 2021 and 456.2 mm in 2022.

Preparation of Laser trilobum Extract and Synthesis of AgNPs

The elimination of surface contaminants and physically adsorbed particles from the gathered seeds was achieved using a sequential rinsing process involving tap water and subsequently deionized water. Subsequently, the seeds were subjected to a desiccated environment devoid of moisture and dried for 5 days while being kept in a shady area. Subsequently, the substance was meticulously pulverized using a grinder.

Three different extracts were obtained by adding 10 g of *L. trilobum* powder to a flask containing 100 mL of deionized water and refluxing at 80 °C for 60, 120, and 180 min (Jadhav et al., 2015). The extracts were filtered through Whatman No. 1 filter paper and stored at 4 °C until further analysis.

L. trilobum extracts (1 mL) prepared as described above were mixed with 10 mL of aqueous $AgNO_3$ solutions prepared at three different concentrations (1, 3, and 5 mM). The reaction mixtures were set aside for 24 h at three different temperatures: 25, 45, and 65 °C. A red-brown color was observed in the mixture after 24 h, confirming the formation of AgNPs (Behravan et al., 2019). Colloidal AgNPs were centrifuged at 10,000 rpm for 15 min and washed twice with distilled water. The obtained AgNPs were dried in an oven at 40 °C overnight.

Experimental Design

The AgNP synthesis conditions were optimized using response surface methodology (RSM). A Box–Behnken design (BBD) with three levels and three factors was employed to optimize the extraction time (X1), $AgNO_3$ concentration (X2), and synthesis temperature (X3) to obtain the most favorable outcome in terms of inhibition zone diameters. The independent variables are listed in Table S1. This design was at three levels with 15 runs including three times in central point. The experimental design is summarized in Table S2. The fruits of *L. trilobum* harvested in different years were optimized for their own year. The experimental data acquired from BBD were analyzed using regression and fitted to a second-order polynomial Eq. (1) to clarify the relationship between the antibacterial activity of AgNPs and various variables (Veza et al., 2023).

$$Z = \beta_0 + \sum_{i=l}^{2} \beta_i X_i + \sum_{i=l}^{2} \beta_{ii} X_i^2 + \sum_{i=l}^{1} \sum_{j=i+l}^{2} \beta_{ij} X_i X_j \quad (1)$$

where Z represents the predicted response (antimicrobial activity yield of AgNPs); β_0, β_i, β_{ii}, and β_{ij} are the regression coefficients for the intercept, linear, quadratic, and interaction, respectively; n is the number of variables; and X_i and X_j are independent variables influencing the response.

Characterization of AgNPs

The experimental solutions were prepared using ultrapure water sourced from Arium® Pro VF Ultrapure water system. Centrifugation was performed using a Hettich Universal 320 centrifuge. The absorption spectra of the AgNPs were recorded using a UV–Vis spectrometer (PG Instruments TG 60) in the wavelength range of 300–800 nm. A Memmert UN 110 drying oven was used to dry the AgNPs. The morphologies and particle sizes of the silver nanoparticles (AgNPs) were examined using a transmission electron microscope (TEM) (model Hitachi HT7800). FTIR spectroscopy (Perkin Elmer Fronter) in the scanning range of 4000–400 cm^{-1} (scan speed of 4 cm^{-1}) at room temperature was used to distinguish and characterize the functional groups present in both the *L. trilobum* extract and the AgNPs. The crystal structures of the AgNPs were determined using a Bruker AXS D8 X-ray diffractometer. The measurements were conducted at a voltage of 40 kV and current of 40 mA, with a 2θ scanning range of 10–90°.

Disc Diffusion Tests

Each bacterial strain was grown on Tryptic Soy Agar for 18 h at 37 °C. The turbidity of the bacteria was adjusted to 0.5 McFarland via a densitometer (Biosan, Latvia) in 0.9% NaCl. 100 µL of bacterial suspension in 0.9% NaCl was inoculated onto the surface of Mueller–Hinton Agar Petri plates using a swab. After impregnating 6 mm sterile discs (Whatman™ 2017–006) with 30 µL of AGNP, the discs were placed on petri dishes, and the microorganisms were incubated at 37°C for 48 h. The diameters of the inhibition zones at the end of the incubation period were measured using a millimeter ruler (CLSI 2021). Aqueous extracts without nanoparticles were used as negative controls (Soyuçok et al., 2023).

Determination of Minimum Inhibitory Concentration (MIC) Value

A 200 µL of Muller–Hinton II Broth containing AgNPs (at 0.63, 1.25, 2.50, 5.00, 10.00, 20.00, and 40.00 µg/mL) was added directly to a 96-well plate, and 20 µL of bacterial suspension was mixed into Muller–Hinton II containing AgNPs. Muller–Hinton II Broth without AgNP was used as a control. The plates were then incubated at 37 °C for 24 h (Schug et al., 2020). The absorbance of the wells was determined at 600 nm using a spectrophotometer (Varioskan Lux, Thermo, Finland). The analysis was performed in triplicate.

Determination of Minimum Bactericidal Concentration (MBC) Values

After incubation, 10 µL of the suspension was added to each well and inoculated on fresh TSA plates. TSA plates were incubated at 37 °C for 24 h, and the lowest AgNP concentration that completely inhibited bacterial growth was determined as the MBC value. MBC is the lowest concentration that kills 100% of the bacterial load and does not result in any viable growth on agar plates (Soyuçok et al., 2023).

Statistical Analyses

The results were analyzed using the Minitab Statistical Package Program (Minitab® 19.1.1 (64-bit)) (Minitab, State College, PA) and fitted to a full quadratic regression equation (with coefficients of linear, quadratic, and two-factor interaction effects). The relevant responses were the inhibition zone diameter of each nanoparticle against *S. aureus*, *S.* Typhimurium, *E. coli*, and *L. monocytogenes* were maximized. The coefficient of determination (R^2) and adjusted coefficient of determination (R^2 adj) were determined using the Minitab statistical package. The surfaces were drawn using the Minitab statistical package. In addition to the optimization study, the inhibition zone diameter results were compared statistically for each year, and the significance levels ($p < 0.05$) of the differences were determined. For this purpose, analysis of variance (ANOVA) with Tukey's test was performed using the Minitab statistical package ($p < 0.05$). Results are expressed as mean ± standard deviation of the mean.

Results and Discussion

Antimicrobial Optimization

For the antimicrobial tests, AgNPs were synthesized considering the 15 runs given in Table S1. The inhibition diameters of the AgNPs synthesized using the Box–Behnken experimental design to determine the AgNPs with the highest antimicrobial effect are listed in Table 1. The maximum and minimum inhibition zone diameters for *S. aureus*, *S.* Typhimurium, *E. coli*, and *L. monocytogenes* in AgNP L_{21} particles were calculated as 6.0–15.0 mm, 7.0–15.0 mm, 6.0–16.0 mm, and 6.0–14.0 mm, respectively (Fig. S1). In AgNP L_{22} particles, the maximum and minimum inhibition zone diameters of *S. aureus*, *S.* Typhimurium, *E. coli*, and *L. monocytogenes* were found to be 6.0–15.0 mm, 6.0–14.5 mm, 8.0–16.0 mm, and 6.0–14.5 mm, respectively.

The parameters and regression coefficients of the developed models for each nanoparticle are presented in Table 2. Except for *L. monocytogenes* (> 68%), the results revealed that the models produced for *S. aureus*, *S.* Typhimurium, and *E. coli* for each particle displayed high performance in explaining their changes, depending on the synthesis parameters. These models explained more than 84.00%, 81.00%, and 89.00% of the variation in the antimicrobial activities of *S. aureus*, *S.* Typhimurium, and *E. coli*, respectively (Tables S3-S4). Evaluation of the significance of the model parameters showed that the first-order extraction time term was significant for the inhibition zone diameter of *S. aureus* by 2022. The second-order concentration was significant for the inhibition zone diameters of *S. aureus* and *S.* Typhimurium by 2022. The interaction term between the concentration and extraction time was significant for the inhibition zone diameter of *S. aureus* by only 2022. The second-order extraction time was significant for the inhibition zone diameter of *S.* Typhimurium only 2022.

Variables: β_0 is the constant coefficient; β_i is the linear coefficient (main effect); β_{ii} is the quadratic coefficient; β_{ij} is the two factors' interaction coefficient. *ns* not significant ($p > 0.05$); *significant at $p \leq 0.05$; **significant at $p \leq 0.01$; ***significant at $p \leq 0.001$—the values with a significance

Table 1 Dependent variables used in the optimization process; zone diameters formed by the tested bacteria

	2021				2022			
Run order	*S. aureus*	*S.* Typhimurium	*E. coli*	*L. monocytogenes*	*S. aureus*	*S.* Typhimurium	*E. coli*	*L. monocytogenes*
1	9.5	11.5	11.5	6.0	11.0	11.0	11.5	9.0
2	15.0	14.0	16.0	14.0	14.5	14.5	16.0	14.5
3	6.0	8.5	8.0	6.0	9.0	10.0	10.5	9.0
4	12.5	13.5	15.0	11.0	13.0	14.0	15.0	13.5
5	6.0	7.0	6.0	6.0	6.0	6.0	8.0	6.0
6	6.0	7.0	6.0	6.0	6.0	6.0	9.0	6.0
7	6.0	8.5	10.5	6.0	6.0	6.0	10.0	11.0
8	13.0	14.0	15.5	14.0	13.0	13.5	13.0	11.0
9	11.0	11.0	13.0	11.0	10.5	12.0	12.0	6.0
10	8.0	8.0	9.0	6.0	8.0	11.5	13.0	6.0
11	14.0	13.7	14.0	14.0	11.0	14.5	14.0	13.0
12	6.0	8.0	9.0	8.0	14.0	9.0	10.0	6.0
13	6.0	7.5	8.0	6.0	10.0	11.0	11.0	6.0
14	13.0	15.0	14.0	14.0	15.0	14.5	15.0	14.0
15	8.0	11.0	13.0	9.0	10.0	11.0	10.5	6.0

Table 2 Coefficients and lack-of-fit values of models

	2021				2022			
Variables	*S. aureus*	*S.* Typhimurium	*E. coli*	*L. monocytogenes*	*S. aureus*	*S.* Typhimurium	*E. coli*	*L. monocytogenes*
β_0	9.333***	10.547***	11.233***	9.133***	9.429**	11.269***	11.900***	9.133***
β_1	-	-	-	-	−1.625*	−0.563 ^{ns}	−0.563 ^{ns}	
β_2	2.375***	2.150***	2.438***	2.375**	1.375*	1.313**	1.687***	3.188***
β_3	−3.438***	−2.750***	−3.500***	−3.000**	−2.375**	−3.375***	−2.375***	−2.000**
β_{11}	-	-	-	-	1.946*	1.154*	-	-
β_{12}	-	-	-	-	-	-	-	-
β_{13}	-	-	-	-	−2.000*	-	-	-
β_{21}	-	-	-	-	-	-	-	-
β_{22}	-	-	-	-	-	-	-	-
β_{23}	-	-	-	-	-	-	-	-
β_{31}	-	-	-	-	-	-	-	-
β_{32}	-	-	-	-	-	-	-	-
β_{33}	-	-	-	-	-	−1.721**	-	-
Model	***	***	***	***	**	***	***	***
R^2	85.24	81.60	89.32	68.20	84.98	93.47	89.62	69.83
Adj R^2	82.78	78.54	87.54	62.90	76.63	89.83	86.78	64.8
Lack of fit	0.274	0.41	0.958	1.62	0.611	0.065	0.890	0.480

level less than 0.05 were removed from the model using backward elimination.

For 2021 and 2022, a three-dimensional image of the change in the inhibition zone diameter process parameters was produced using a pairwise combination of the three factors (Figs. 1 and 2). Our results showed that the inhibition zone diameters with the $AgNO_3$ concentration and synthesis temperature were consistent with the significance of the corresponding model terms in 2021. As shown in Fig. 1, the effects of temperature and time on the diameter of the inhibition zone were clear.

A strong effect of first-order terms is observed in Fig. 2. The inhibition zone diameters of *S. aureus* and *S.* Typhimurium increased with increasing $AgNO_3$ concentration and decreasing extraction time (Fig. 2a, b). Unlike the inhibition zone diameters of *S. aureus* and *S.* Typhimurium, $AgNO_3$

Fig. 1 Influence of independent variables in AgNPs L_{21} inhibition zone diameter of **a** *S. aureus*, **b** *S.* Typhimurium, **c** *E. coli*, and **d** *L. monocytogenes*

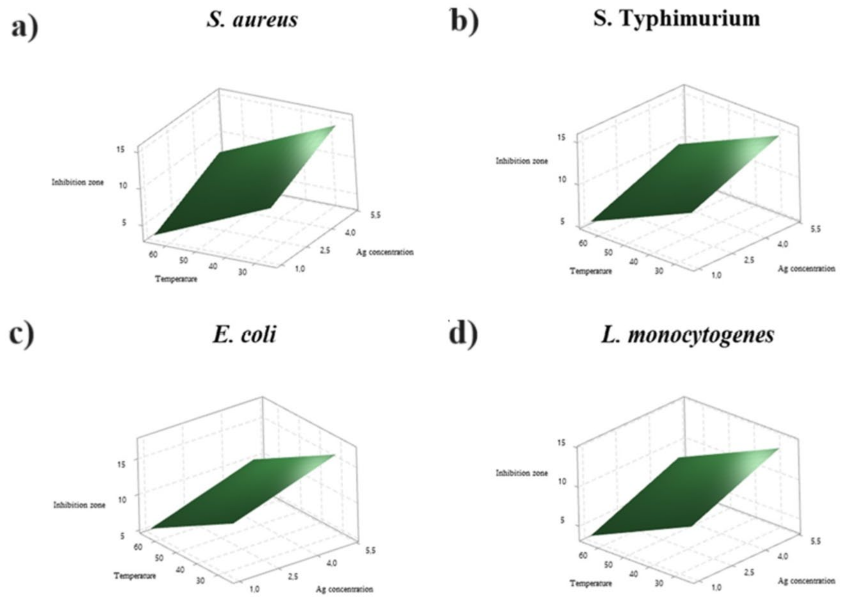

2021

Fig. 2 Influence of independent variables in AgNPs L_{22} inhibition zone diameter of **a** *S. aureus*, **b** *S.* Typhimurium, **c** *E. coli*, and **d** *L. monocytogenes*

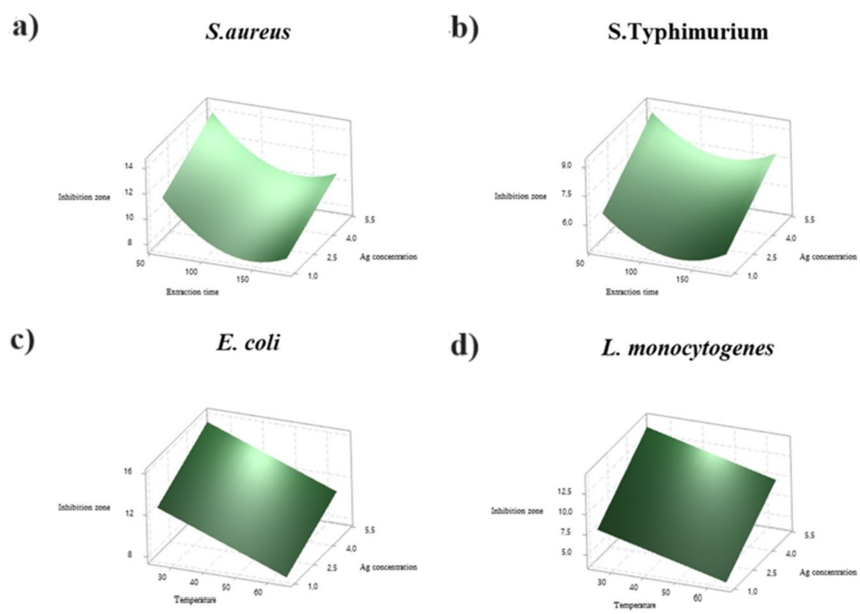

2022

concentration and temperature clearly affected the variation in the inhibition zone diameters of *E. coli* and *L. monocytogenes* (Fig. 2c, d).

After analyzing the findings depicted in Figs. 1 and 2, it is evident that a decrease in the synthesis temperature and an increase in the silver concentration led to an observed increase in antibacterial activity. When the literature is examined, it is concluded that the volume of nanoparticles will increase owing to the conversion of Ag^+ to Ag^0, especially at high concentrations, and this will have a positive effect on antimicrobial activity (Behravan et al., 2019; Shameli et al., 2011; Dubeya et al., 2010). In particular, lower temperatures allow for better control over the reaction and nucleation rates, resulting in more uniform and controlled nanoparticle formation (Naghmachi et al., 2022; Rosman et al., 2020; Trak & Arslan, 2021; Zhang et al., 2019).

The obtained data were statistically evaluated and dependent variables with high predictive power were

Table 3 Optimal synthesis conditions for each year

	2021	2022
Extraction time (min)	ns	60
$AgNO_3$ concentration (mM)	5	5
Temperature (°C)	25	25

maximized during the optimization process. Under these conditions, the optimal nanoparticle synthesis conditions are listed in Table 3.

ns not significant.

Our study shows that nanoparticle synthesis has been successfully optimized and validated. Our results remained within the theoretical and experimental confidence intervals, and the analyses were successfully validated (Table 4). According to the harvest year, the difference in inhibition zone diameter was not statistically significant (Table 5). This mention supports our hypotheses. Our study showed that the nanoparticle synthesis was successfully optimized and validated.

Characterization of AgNPs

Characterization of AgNPs was carried out using the extract of the *L. trilobum* plant (2021 and 2022 harvest) with the green synthesis method using AgNPs that showed the best antimicrobial activity against the tested bacteria. AgNPs were prepared by adding 5 mM $AgNO_3$ (10 mL) solution to the extracts (1 mL) obtained with a reflux time of 60 min and maintaining them at room temperature (25 °C) for 24 h.

Typically, the initial confirmation of AgNP generation is the change in color observed inside the reaction medium (see inset in Fig. 3a L. *trilobum* extract and b AgNPs). The literature has pointed out that the observed surface plasmon resonance (SPR) band of silver nanoparticles (AgNPs) can be detected within the wavelength range of 400–500 nm in UV–Vis spectra. The presence of the SPR peak at 428 nm (Fig. 3) confirmed the formation of AgNPs (Huong & Thang, 2021; Sivaramakrishnan et al., 2019).

The TEM measurements were conducted using grids prepared from solutions containing nanoparticles. In this process, a small volume of the nanoparticle solution, synthesized under ideal conditions, was applied to a 200-mesh copper grid coated with a layer of carbon. Subsequently, the grid was allowed to air-dry overnight under ambient conditions. The surface morphology and size distribution of the synthesized green AgNPs were determined by TEM measurements using the ImageJ Analyzer software. High-resolution TEM images (Fig. 4a, c) revealed that the nanoparticles had small sizes, a smooth surface without aggregation, and a spherical morphology. Based on the size distribution histogram (Fig. 4b, d), it was determined that both the 2021 and 2022 AgNPs had sizes below 100 nm (within the size range of 12.5–47.5 nm) and had an average particle size of 30 ± 12 nm. In both cases, the AgNPs were coated with a thin biotic layer that served as a capping and reducing agent. The obtained results revealed that the particle sizes of the AgNPs were in good agreement with those in the literature (Farnad & Farhadi, 2023; Hashemi et al., 2022; Maciel et al., 2020; Mahapatra et al., 2022; Malaikozhundan et al., 2017).

Table 5 Inhibition zone diameters of nanoparticles produced under optimized conditions

	S. aureus	*S.* Typhimurium	*E. coli*	*L. monocytogenes*
2021	14.10 ± 0.14[a]	14.35 ± 0.50[a]	15.75 ± 0.35[a]	13.25 ± 0.35[a]
2022	14.50 ± 0.71[a]	15.75 ± 0.35[a]	15.35 ± 0.50[a]	13.60 ± 0.14[a]

[a]Mean with the same letter in the same column is not statistically significant ($p > 0.05$)

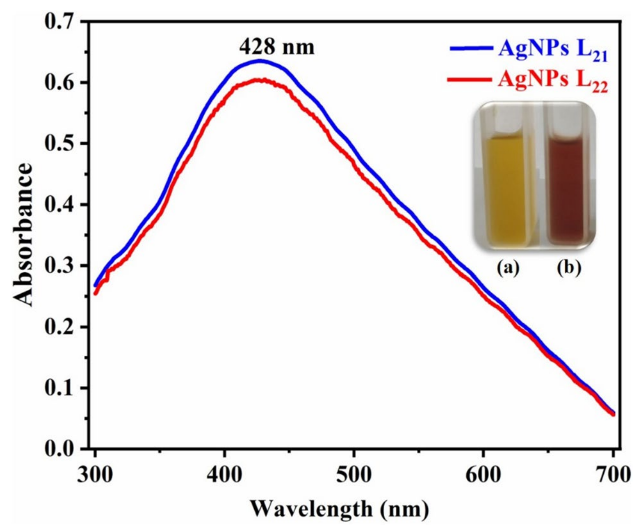

Fig. 3 UV–Vis absorption spectra of green synthesised AgNPs

Table 4 Theoretical and experimental confidence intervals of inhibition zone diameters

	Year	*S. aureus*	*S.* Typhimurium	*E. coli*	*L. monocytogenes*
Theoretical	2021	(13.406; 16.886)	(13.787; 17.106)	(15.694; 18,647)	(11.89; 17.12)
	2022	(11.85; 17.65)	(14.276; 17.628)	(15.265; 17.785)	(11.84; 16.80)
Experimental	2021	14.35	14.1	15.75	13.25
	2022	15.75	14.5	15.35	13.6

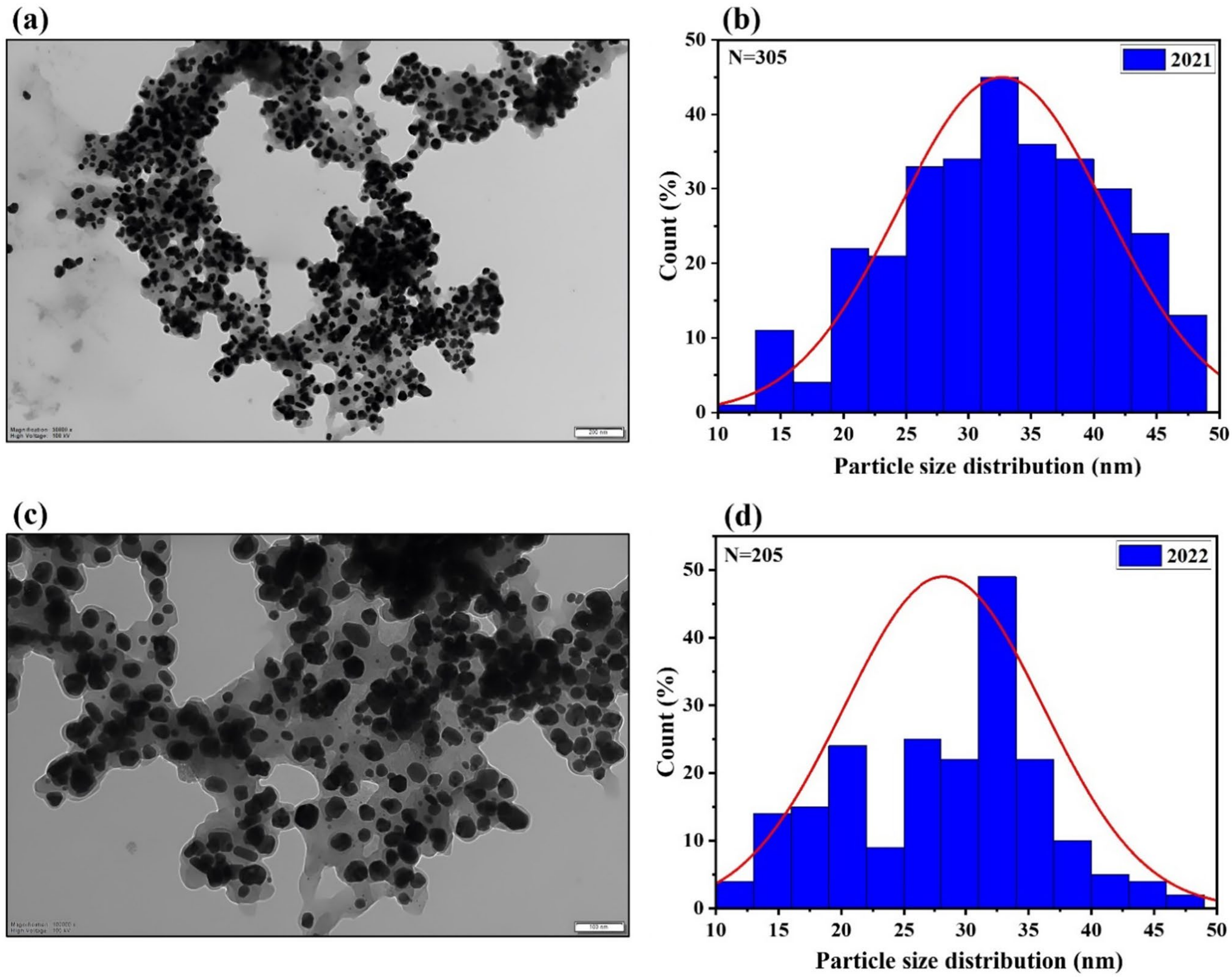

Fig. 4 TEM images (**a**, **c**) at two magnifications (×50,000, ×100,000) and size distribution histogram (**b**, **d**) for AgNPs

The crystal structures of the synthesized AgNPs were determined by XRD. For this, AgNPs synthesized under optimal conditions were centrifuged at 10,000 rpm for 15 min, washed twice with distilled water, and dried overnight in an oven at 40 °C. The XRD spectra of the solid AgNPs are shown in Fig. 5. The XRD pattern showed a centered cubic face (FCC) crystal structure for both the synthesized AgNPs. The AgNPs showed four characteristic peaks at 38.11°, 44.01°, 65.01°, and 77.01°, which were assigned to the diffraction signals of the (111), (200), (220) and (311) planes, respectively. Crystallinity calculations using the XRD pattern with OriginPro software showed that the 2021 and 2022 AgNPs had crystal structures of 52% and 50%, respectively. In addition, the observed diffraction peaks matched the Joint Standard Committee on Diffraction data (JCPDS PDF no. 01–087-0717) (Bhanumathi et al., 2018).

To identify the potential functional groups responsible for the generation of AgNPs, FTIR studies were conducted

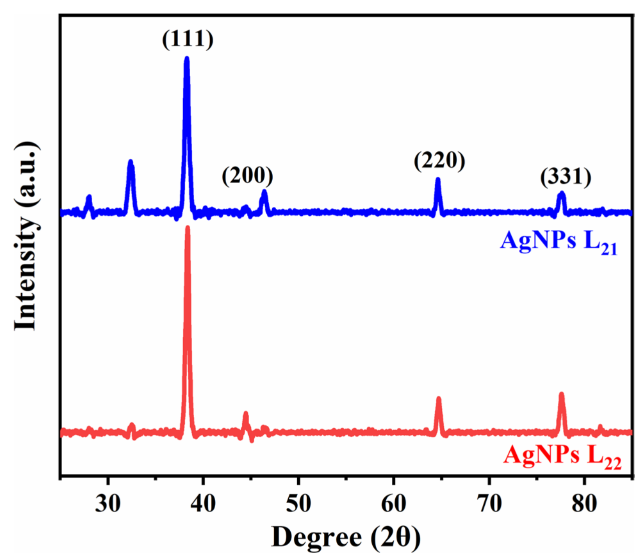

Fig. 5 XRD patterns of AgNPs synthesized under optimal conditions

on both the *L. trilobum* extract and the synthesized AgNPs (dried). For this purpose, extracts of the 2021 and 2022 *L. trilobum* fruits were obtained separately. The obtained extracts were synthesized as 2021 and 2022 AgNPs using the procedure described in the AgNP synthesis section. Figure 6a and b shows the FTIR spectra of 2021 and 2022 extracts and AgNPs, respectively. As shown in Figs. 5 and 6, the FTIR spectra of both extracts and AgNPs of 2021 and 2022 products were very similar to each other. This suggests that very stable AgNPs can be produced using a *L. trilobum* fruit under the proposed experimental conditions. The prominent functional group vibrations of 2021 and 2022 extracts included O–H or N–H (3300 cm^{-1}), C≡C or C≡N (2333, 2315 cm^{-1}), alkenyl C = C of the aromatic ring, or C = O of the amide group stretching vibration (1633 cm^{-1}) and C-H (1400 cm^{-1}) (Alhaidrai et al., 2022; Basu et al., 2015; Chinnathambi et al., 2023; Schmidt et al., 2023; Sivaramakrishnan et al., 2019; Wang et al., 2023). These characteristic peaks in the *L. trilobum* extract spectrum confirmed the presence of saponins, flavonoids, and oligosaccharides, which may function as reducing and stabilizing agents in plant extracts. Following the reduction reaction and subsequent purification, comparable absorption peaks at approximately 3224 cm^{-1} (O–H/N–H); 2918 and 2848 cm^{-1} (C-H); 1631 cm^{-1} (C = C/C = O); 1512 and 1375 cm^{-1} (C–C); and 1020 cm^{-1}(C-N) revealed the existence of residual organic molecules on the surface of the AgNPs (Chinnathambi et al., 2023; Huong & Thang, 2021; Ramar et al., 2015; Schmidt et al., 2023; Wang et al., 2023). However, the significant decrease in the intensity of the peaks at 3224–3227 cm^{-1} and 1600 cm^{-1} in the AgNP samples suggests that flavonoids and saponins in the extract structure are involved in the reduction process.

MIC and MBC Value

In this study, the MIC and MBC values of AgNPs L_{21} and AgNPs L_{22} were determined against tested bacteria. The MIC value of AgNPs L_{21} and AgNPs L_{22} was 10 µg/mL for all tested bacteria. The MBC value for tested bacteria except for *S. aureus* was 20 µg/mL but for *S. aureus*, was 10 µg/mL (Table 6).

Silver ions are responsible for antibacterial effects of silver nanoparticles. Silver ions are released from silver nanoparticles in an aqueous medium. Due to bigger surface area, silver nanoparticles show a stronger and better bactericidal effect (Parvekar et al., 2020). The fundamentals of main bactericidal effects of AgNPs were interfered with the integrity of the bacterial cell by binding to essential cellular structure (Afhkami et al., 2021), particularly to their SH groups (Zhou et al., 2012); generate reactive oxygen species and free radicals which damage the bacterial cell wall; inhibit the respiratory enzymes; and disturb the DNA replication. AgNPs have biocidal properties against various bacteria (Prabhu & Poulose, 2012), and Ruparelia et al. (2008) reported that Ag and Cu nanoparticle showed antimicrobial activity against *E. coli*, *S. aureus*, and *Bacillus subtilis*. Researchers revealed that the MIC and MBC value of Ag nanoparticle for *S. aureus* and *E. coli* was 120–160 µg/mL and 40–60 µg/mL, respectively. Similarly, Parvekar et al. (2020) have reported that the MIC and MBC of silver nanoparticles against *S. aureus* were found to be 0.625 mg/mL. Compared to above result, it has been found that our results were lower than above results. A study performed by Loo et al. (2018) found that the MIC value for *Salmonella*

Table 6 The MIC and MBC values for tested bacteria in each AgNPs (µg/mL)

		S. aureus	*S.* Typhimurium	*E. coli*	*L. monocytogenes*
MIC	AgNPs L_{21}	10	10	10	10
	AgNPs L_{22}	10	10	10	10
MBC	AgNPs L_{21}	20	10	10	10
	AgNPs L_{22}	20	10	10	10

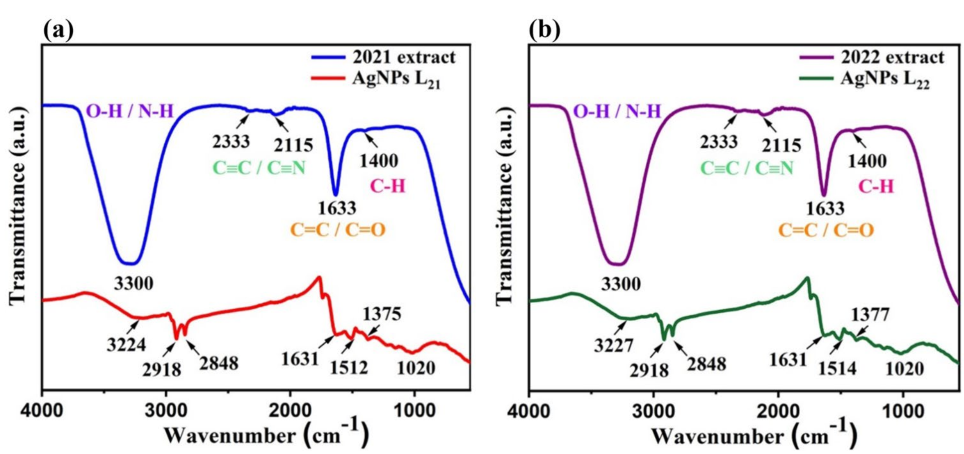

Fig. 6 2021 (**a**) and 2022 (**b**) FTIR spectra of *L. trilobum* extracts and AgNPs

spp. and *E. coli* is 3.9–7.8 µg/mL, respectively. In a study of the antimicrobial activity of Ag nanoparticle on methicillin-resistant *S. aureus* (MRSA), MIC value ranged from 0.5 to 15 µg/mL (Masimen et al., 2022). In our study, *S. aureus* and MRSA show MIC value due to generally the tendency to gain bacterial resistance which is low towards noble metals (Ip et al., 2006).

Ag nanoparticles with grapefruit peel extract showed antimicrobial activity against *E. coli* and *S. aureus*. Researchers stated that the MIC value of this nanoparticle was 0.025 mg/mL and 0.05–0.00625 mg/mL for *E. coli* and *S. aureus* strains, respectively (Arsène et al., 2021). The MBC value of AgNPs with *Tamarix nilotica* against *L. monocytogenes* ATCC 19114, *L. monocytogenes* ATCC 13932, and *Listeria innocua* ATCC 33090 was 32, 64, and 32 µg/mL, respectively. Moreover, researchers report that the MIC value of AgNPs with *Tamarix nilotica* against *L. monocytogenes* strains ranged from 16 to 32 µg/mL while for *L. innocua*, the MIC value was 16 µg/mL (Al-Shabib et al., 2020). In other study, AgNP with ananas peel extract demonstrated 50 µg/mL MIC and 100 µg/mL MBC value for *L. monocytogenes* (Das et al., 2019). AgNPs with *Murraya koenigii* aqueous extract exhibited 32 µg/mL MIC value for MRSA, 16 µg/mL for *E. coli*, and 64 µg/mL for beta lactam–resistant *E. coli* (Qais et al., 2019). Carson et al. (2020) reported that AgNPs with *Phyla dulcis* extract were found effective against drug-resistant *S.* Typhimurium, *S. aureus*, *E. coli* O157:H7, and *L. monocytogenes*. The MIC value of the AgNPs with *Angelica keiskei* was found and 12.5 µg/mL for *L. monocytogenes* (Du et al., 2019).

Conclusion

Nanoparticle synthesis typically involves low temperatures and short time periods. However, it is important to optimize certain parameters, such as metal concentration, synthesis time, extraction time, synthesis temperature, harvest time, and environmental factors, owing to the variations in the biological materials used in green synthesis. In this study, the silver concentration, extraction time, and temperature, which are the most important factors affecting nanoparticle synthesis, were optimized. Owing to the RSM technique used, traditional synthesis studies, which require a long time and are costly, have become easier. The most striking point of this study was that the synthesis conditions were created according to the highest antimicrobial activity. Based on the analyses conducted, it was shown that the synthesis temperature had a negative impact on the antibacterial activity of AgNPs, whereas the silver concentration had a positive impact on the activity. The characterization results of AgNPs synthesized using the aqueous extract of *L. trilobum* harvested in different years, which were optimized for antimicrobial activity, did not differ for AgNPs L_{21} and L_{22}. Furthermore, there was no observed significant alteration in the antibacterial efficacy of the harvest year on the tested bacteria. In summary, the optimized synthesis of AgNPs from *Laser trilobum* extracts represents a valuable advancement in the field of antimicrobial nanotechnology. The future application areas of this work encompass the food science and industry, healthcare, and environmental sectors, where these nanoparticles have the potential to enhance biocontrol measures, mitigate bacterial contamination, and contribute to improved public health and environmental sustainability.

Supplementary Information The online version contains supplementary material available at https://doi.org/10.1007/s11947-024-03359-3.

Acknowledgements The authors would like to thank the coordinators of the projects organized by the Scientific and Technological Research Council of Turkey ("TÜBİTAK 2237-A, Proses Analizi ve Optimizasyonu"; Project Number: 1129B372201396) for their help in calculations.

Author Contributions A.S.: conceptualization, data curation, formal analysis, investigation, methodology, software, validation, visualization, and writing original draft. B.K.: conceptualization, data curation, formal analysis, investigation, methodology, software, visualization, and writing original draft. B.T.: conceptualization, data curation, formal analysis, investigation, methodology, and writing original draft. All authors read and approved the final manuscript.

Funding Open access funding provided by the Scientific and Technological Research Council of Türkiye (TÜBİTAK).

Data Availability No datasets were generated or analyzed during the current study.

Declarations

Competing Interests The authors have no conflict of interest.

References

Abdi, M. R., Ghalandarzadeh, A., & Shafiei-Chafi, L. (2022). Optimization of lime and fiber content for improvement of clays with different plasticity using response surface method (RSM). *Transportation Geotechnics, 32*, 100685. https://doi.org/10.1016/j.trgeo.2021.100685

Afhkami, F., Ahmadi, P., Chiniforush, N., & Sooratgar, A. (2021). Effect of different activations of silver nanoparticle irrigants on the elimination of *Enterococcus faecalis*. *Clinical Oral Investigations, 25*, 6893–6899. https://doi.org/10.1007/s00784-021-04351-3

Agarwal, M., Bhadwal, A. S., Kumar, N., Shrivastav, A., Shrivastav, B. R., Singh, M. P., Zafar, F., & Tripathi, R. M. (2016). Catalytic degradation of methylene blue by biosynthesised copper nanoflowers using *F. benghalensis* leaf extract. *IET Nanobiotechnology, 10*, 321–325. https://doi.org/10.1049/iet-nbt.2015.0098

Al Dine, E. J., Ferjaoui, Z., Ghanbaja, J., Roques-Carmes, T., Meftah, A., Hamieh, T., Toufaily, J., Schneider, R., Marchal, S., Gaffet, E., & Alem, H. (2017). Thermo-responsive magnetic Fe_3O_4@P(MEO_2MAX-OEGMA$_{100\text{-}X}$) NPs and their applications as drug delivery systems. *International Journal of Pharmaceutic, 532*, 738–747. https://doi.org/10.1016/j.ijpharm.2017.09.019

Alhaidrai, S. A. A., Al-Hadi, F. A., Al-Kaf, A. G., Al-Deen, A. M. T. (2022). Phytochemical screening by FTIR spectroscopic analysis in the methanolic extracts coffee (*C. arabica. L*) to seeds and peels (unroasted and roasted) cultivars grown in Yemen. *Bioequivalence & Bioavailability International Journal, 6*, 1–8. https://doi.org/10.23880/beba-16000179

Al-Shabib, N. A., Husain, F. M., Nadeem, M., Khan, M. S., Al-Qurainy, F., Alyousef, A. A., Arshad, M., Khan, A., Khan, J. M., Alam, P., Albalawi, T., & Shahzad, S. A. (2020). Bio-inspired facile fabrication of silver nanoparticles from in vitro grown shoots of Tamarix nilotica: Explication of its potential in impeding growth and biofilms of *Listeria monocytogenes* and assessment of wound healing ability. *RSC Advances, 10*, 30139–30149. https://doi.org/10.1039/d0ra04587j

Arsène, M. M., Podoprigora, I. V., Davares, A. K., Razan, M., Das, M. S., Senyagin, A. N. (2021). Antibacterial activity of grapefruit peel extracts and green-synthesized silver nanoparticles. *Veterinary World, 14*, 1330. https://doi.org/10.14202/vetworld.2021.1330-1341

Basu, A., Basu, S., Bandyopadhyay, S., & Chowdhury, R. (2015). Optimization of evaporative extraction of natural emulsifier cum surfactant from *Sapindus mukorossi*—Characterization and cost analysis. *Industrial Crops and Products, 77*, 920–931. https://doi.org/10.1016/j.indcrop.2015.10.006

Batiha, G. E. S., Hussein, D. E., Algammal, A. M., George, T. T., Jeandet, P., Al-Snafi, A. E., ... & Cruz-Martins, N. (2021). Application of natural antimicrobials in food preservation: Recent views. *Food Control*, *126*, 108066. https://doi.org/10.1016/j.foodcont.2021.108066

Baytop, T. (1999). *Geçmişten Bugüne Türkiye'de Bitkiler ile Tedavi*. Istanbul University Publications, https://doi.org/10.26650/AB/AA8.2022.167

Behravan, M., Panahi, A. H., Naghizadeh, A., Ziaee, M., Mahdavi, R., & Mirzapour, A. (2019). Facile green synthesis of silver nanoparticles using *Berberis vulgaris* leaf and root aqueous extract and its antibacterial activity. *International Journal of Biological Macromolecules, 124*, 148–154. https://doi.org/10.1016/j.ijbiomac.2018.11.101

Bhanumathi, R., Manivannan, M., Thangaraj, R., & Kannan, S. (2018). Drug-carrying capacity and anticancer effect of the folic acid- and berberine-loaded silver nanomaterial to regulate the AKT-ERK pathway in breast cancer. *ACS Omega, 3*, 8317–8328. https://doi.org/10.1021/acsomega.7b01347

Carson, L., Bandara, S., Joseph, M., Green, T., Grady, T., Osuji, G., Weerasooriya, A., Ampim, P., & Woldesenbet, S. (2020). Green synthesis of silver nanoparticles with antimicrobial properties using *Phyla dulcis* plant extract. *Foodborne Pathogens and Disease, 17*, 504–511. https://doi.org/10.1089/fpd.2019.2714

Chandhru, M., Logesh, R., Rani, S. K., Ahmed, N., & Vasimalai, N. (2019). One-pot green route synthesis of silver nanoparticles from jack fruit seeds and their antibacterial activities with Escherichia coli and salmonella bacteria. *Biocatalysis and Agricultural Biotechnology, 20*, 101241. https://doi.org/10.1016/j.bcab.2019.101241

Chen, H., Zhoua, J., & Deng, J. (2016). Helical polymer/Fe_3O_4 NPs constructing optically active, magnetic core/shell microspheres: Preparation by emulsion polymerization and recycling application in enantioselective crystallization. *Polymer Chemistry, 7*, 125–134. https://doi.org/10.1039/C5PY01549A

Chinnathambi, A., Alharbi, S. A., Joshi, D., Saranya, V., Jhanani, G. K., On-uma, R., Jutamas, K., & Anupong, W. (2023). Synthesis of AgNPs from leaf extract of *Naringi crenulata* and evaluation of its antibacterial activity against multidrug resistant bacteria. *Environmental Research, 216*, 114455. https://doi.org/10.1016/j.envres.2022.114455

Cianfaglione, K., Blomme, E. E., Quassinti, L., Bramucci, M., Lupidi, G., & Dall'Acqua, S., Maggi, F. (2017). Cytotoxic essential oils from Eryngium campestre and Eryngium amethystinum (Apiaceae) growing in central Italy. *Chemistry & Biodiversity, 14*(7), e1700096. https://doi.org/10.1002/cbdv.201700096

Das, G., Patra, J. K., Debnath, T., Ansari, A., Shin, H. S. (2019). Investigation of antioxidant, antibacterial, antidiabetic, and cytotoxicity potential of silver nanoparticles synthesized using the outer peel extract of *Ananas comosus (L.)*. *Plos One, 14*(8), e0220950. https://doi.org/10.1371/journal.pone.0220950

Du, J., Hu, Z., Dong, W. J., Wang, Y., Wu, S., & Bai, Y. (2019). Biosynthesis of large-sized silver nanoparticles using *Angelica keiskei* extract and its antibacterial activity and mechanisms investigation. *Microchemical Journal, 147*, 333–338. https://doi.org/10.1016/j.microc.2019.03.046

Dubeya, S. P., Lahtinen, M., & Sillanpää, M. (2010). Tansy fruit mediated greener synthesis of silver and gold nanoparticles. *Process Biochemistry, 45*, 1065–1071. https://doi.org/10.1016/j.procbio.2010.03.024

Facciola, S. (1990). *Cornucopia—A source book of edible plants*. Kampong Publications.

Farnad, N., & Farhadi, K. (2023). Introducing potato starch-ecofriendly silver nanoparticles as a novel binary system for nanoencapsulation of riboflavin. *Food Chemistry, 398*, 133910. https://doi.org/10.1016/j.foodchem.2022.133910

Hajji, M., Falcimaigne-Gordin, A., Ksouda, G., Merlier, F., Thomasset, B., & Nasri, M. (2021). A water-soluble polysaccharide from Anethum graveolens seeds: Structural characterization, antioxidant activity and potential use as meat preservative. *International Journal of Biological Macromolecules, 167*, 516–527. https://doi.org/10.1016/j.ijbiomac.2020.12.006

Hashemi, Z., Mizwari, Z. M., Mohammadi-Aghdam, S., Mortazavi-Derazkola, S., & Ebrahimzadeh, M. A. (2022). Sustainable green synthesis of silver nanoparticles using *Sambucus ebulus* phenolic extract (AgNPs@SEE): Optimization and assessment of photocatalytic degradation of methyl orange and their in vitro antibacterial and anticancer activity. *Arabian Journal of Chemistry, 15*(1), 103525. https://doi.org/10.1016/j.arabjc.2021.103525

He, Y., Xie, Y., Huang, Y., Xia, D., Zhang, Y., Liu, Y., Xiao, Y., Shen, F., He, J., & Luo, L. (2022). Optimization of cyanobacteria *Microcystis aeruginosa* extract to improve the yield of Ag nanoparticles with antibacterial property. *International Biodeterioration & Biodegradation, 171*, 105407. https://doi.org/10.1016/j.ibiod.2022.105407

Hoseinpour, V., & Ghaemi, N. (2018). Green synthesis of manganese nanoparticles: Applications and future perspective–A review. *Journal of Photochemistry and Photobiology B, 189*, 234–243. https://doi.org/10.1016/j.jphotobiol.2018.10.022

Huong, V. T. L., & Thang, N. N. (2021). Green synthesis, characterization and antibacterial activity of silver nanoparticles using *Sapindus mukorossi* fruit pericarp extract. *Materials Today:*

Proceedings, 42, 88–93. https://doi.org/10.1016/j.matpr.2020.10.015

Ip, M., Lui, S., Poon, V. K., Lung, I., & Burd, A. (2006). Antimicrobial activities of silver dressings: An in vitro comparison. *Journal of Medical Microbiology, 55*, 59–63. https://doi.org/10.1099/jmm.0.46124-0

Jadhav, K., Dhamecha, D., Dalvi, B., & Patil, M. (2015). Green synthesis of silver nanoparticles using *Salacia chinensis*: Characterization and its antibacterial activity. *Particulate Science and Technology, 33*, 445–455. https://doi.org/10.1080/02726351.2014.1003628

Khan, S., Khan, K., Qi, I., Wu, F., Gao, D., Humayum, M., Khan, A., Bahadur, A., Alanazi, A. F., & Bououdina, M. (2023). Eco-friendly graphitic carbon nitride nanomaterials for the development of innovative biomaterials: Preparation, properties, opportunities, current trends, and future outlook. *Journal of Saudi Chemical Society, 27*(6), 101753. https://doi.org/10.1016/j.jscs.2023.101753

Kivanc, M., & Akgül, A. (1991). Effect of *Laser trilobum* spice on natural microflora of köfte, a Turkish ground meat product. *Food/nahrung, 35*(2), 149–154. https://doi.org/10.1002/food.19910350206

Loo, Y. Y., Rukayadi, Y., Nor-Khaizura, M. A. R., Kuan, C. H., Chieng, B. W., Nishibuchi, M., & Radu, S. (2018). In vitro antimicrobial activity of green synthesized silver nanoparticles against selected gram-negative foodborne pathogens. *Frontiers in Microbiology, 9*, 1555. https://doi.org/10.3389/fmicb.2018.01555

Ma, Y., Yang, J., Hu, Y., Xia, Z., & Cai, K. (2022). Osteogenic differentiation of the MSCs on silk fibroin hydrogel loaded Fe_3O_4@PAA NPs in static magnetic field environment. *Colloids and Surfaces b: Biointerfaces, 220*, 112947. https://doi.org/10.1016/j.colsurfb.2022.112947

Maciel, M. V. O. B., Almeida, A. R., Machado, M. H., Elias, W. C., Rosa, C. G., Teixeira, G. L., Noronha, C. M., Bertoldi, F. C., Nunes, M. R., Armas, R. D., & Barreto, P. L. M. (2020). Green synthesis, characteristics and antimicrobial activity of silver nanoparticles mediated by essential oils as reducing agents. *Biocatalysis and Agricultural Biotechnology, 28*, 101746. https://doi.org/10.1016/j.bcab.2020.101746

Mahapatra, A. D., Patra, C., Pal, K., Mondal, J., Sinha, C., & Chattopadhyay, D. (2022). Green synthesis of AgNPs from aqueous extract of Oxalis corniculata and its antibiofilm and antimicrobial activity. *Journal of the Indian Chemical Society, 99*(7), 100529. https://doi.org/10.1016/j.jics.2022.100529

Mahmud, J. R., & Khan, A. (2018). Characterization of natural antimicrobials in food system. *Advances in Applied Microbiology, 8*, 894–916. https://doi.org/10.4236/aim.2018.811060

Mahmud, J., Muranyi, P., Salmieri, S., & Lacroix, M. (2023). Optimization of a natural antimicrobial formulation against potential meat spoilage bacteria and food-borne pathogens: Mixture design methodology and predictive modelling. *Microbial Pathogenesis, 176*, 106000. https://doi.org/10.1016/j.micpath.2023.106000

Malaikozhundan, B., Vijayakumar, S., Vaseeharan, B., Jenifer, A. A., Chitra, P., Prabhu, N. M., & Kannapiran, E. (2017). Two potential uses for silver nanoparticles coated with *Solanum nigrum* unripe fruit extract: Biofilm inhibition and photodegradation of dye effluent. *Microbial Pathogenesis, 111*, 316–324. https://doi.org/10.1016/j.micpath.2017.08.039

Masimen, M. A. A., Harun, N. A., Maulidiani, M., & Ismail, W. I. W. (2022). Overcoming methicillin-resistance *Staphylococcus aureus* (MRSA) using antimicrobial peptides-silver nanoparticles. *Antibiotics, 11*(7), 951. https://doi.org/10.3390/antibiotics11070951

Mohanta, Y. K., Panda, S. K, Syed, A., Ameen, F., Bastia, A. K., Mohanta, T. K. (2018). Bio-inspired synthesis of silver nanoparticles from leaf extracts of Cleistanthus collinus (Roxb.): its potential antibacterial and anticancer activities. *IET Nanobiotechnology*, 12(3),343–348. https://doi.org/10.1049/iet-nbt.2017.0203

Mohanta, Y. K., Biswas, K., Jena, S. K., Hashem, A., Abd_Allah, E. F., & Mohanta, T. K. (2020). Anti-biofilm and antibacterial activities of silver nanoparticles synthesized by the reducing activity of phytoconstituents present in the Indian medicinal plants. *Frontiers in Microbiology* 11:1143. https://doi.org/10.3389/fmicb.2020.01143

Naghmachi, M., Raissi, A., Baziyar, P., Homayoonfar, F., Amirmahani, F., & Danaei, M. (2022). Green synthesis of silver nanoparticles (AgNPs) by *Pistacia terebinthus* extract: Comprehensive evaluation of antimicrobial, antioxidant and anticancer effects. *Biochemical and Biophysical Research Communications, 608*, 163–169. https://doi.org/10.1016/j.bbrc.2022.04.003

Ofgea, N. M., Tura, A. M., & Fanta, G. M. (2022). Activated carbon from H_3PO_4 -activated Moringa Stenopetale Seed Husk for removal of methylene blue: Optimization using the response surface method (RSM). *Environmental and Sustainability Indicators, 16*, 100214. https://doi.org/10.1016/j.indic.2022.100214

Özer, C. O., & Kılıç, B. (2021). Optimization of pH, time, temperature, variety and concentration of the added fatty acid and the initial count of added lactic acid bacteria strains to improve microbial conjugated linoleic acid production in fermented ground beef. *Meat Science, 171*, 108303. https://doi.org/10.1016/j.meatsci.2020.108303

Ozkan, S., Kabak, B., Kenduzler, E. (2023). Optimization effect on green synthesis of silver nanoparticles (AgNPs) using Dimrit raisin extract and their antimicrobial activity. *Journal of the Institute of Science and Technology*, 13(3), 1926–1936. https://doi.org/10.21597/jist.1254243

Parvekar, P., Palaskar, J., Metgud, S., Maria, R., & Dutta, S. (2020). The minimum inhibitory concentration (MIC) and minimum bactericidal concentration (MBC) of silver nanoparticles against Staphylococcus aureus. *Biomaterial Investigations in Dentistry, 7*, 105–109. https://doi.org/10.1080/26415275.2020.1796674

Prabhu, S., Poulose, E. K. (2012). Silver nanoparticles: Mechanism of antimicrobial action, synthesis, medical applications, and toxicity effects. *International Nano Letters*, 2, 1–10. http://www.inl-journal.com/content/2/1/32

Qais, F. A., Shafiq, A., Khan, H. M., Husain, F. M., Khan, R. A., Alenazi, B., Alsalme, A., & Ahmad, I. (2019). Antibacterial effect of silver nanoparticles synthesized using *Murraya koenigii (L.)* against multidrug-resistant pathogens. *Bioinorganic Chemistry and Applications, 2019*, 1–11. https://doi.org/10.1155/2019/4649506dt

Ramar, M., Manikandan, B., Marimuthu, P. N., Raman, T., Mahalingam, A., Subramanian, P., Karthick, S., & Munusamy, A. (2015). Synthesis of silver nanoparticles using *Solanum trilobatum* fruits extract and its antibacterial, cytotoxic activity against human breast cancer cell line MCF 7. *Spectrochimica Acta Part a: Molecular and Biomolecular Spectroscopy, 140*, 223–228. https://doi.org/10.1016/j.saa.2014.12.060

Rashidian, G., Mohammadi-Aloucheh, R., Hosseinzadeh-Otaghvari, F., Chupani, L., Stejskal, V., Samadikhah, H., Zamanlui, S., Multisanti, C. R., & Faggio, C. (2023). Long-term exposure to small-sized silica nanoparticles (SiO_2-NPs) induces oxidative stress and impairs reproductive performance in adult zebrafish (Danio rerio). *Comparative Biochemistry and Physiology Part c: Toxicology & Pharmacology, 273*, 109715. https://doi.org/10.1016/j.cbpc.2023.109715

Rosman, N. S. R., Harun, N. A., Idris, I., & Ismail, W. I. W. (2020). Eco-friendly silver nanoparticles (AgNPs) fabricated by green synthesis using the crude extract of marine polychaete, *Marphysa moribidii*: Biosynthesis, characterisation, and antibacterial applications. *Heliyon, 6*, e05462. https://doi.org/10.1016/j.heliyon.2020.e05462

Ruparelia, J. P., Chatterjee, A. K., Duttagupta, S. P., & Mukherji, S. (2008). Strain specificity in antimicrobial activity of silver and copper nanoparticles. *Acta Biomaterialia, 4*, 707–716. https://doi.org/10.1016/j.actbio.2007.11.006

Schmidt, M. P., Ashworth, D. J., Celis, N., & Ibekwe, A. M. (2023). Optimizing date palm leaf and pistachio shell biochar properties for antibiotic adsorption by varying pyrolysis temperature. *Bioresource Technology, 21*, 101325. https://doi.org/10.1016/j.biteb.2022.101325

Schug, A. R., Bartel, A., Scholtzek, A. D., Meurer, M., Brombach, J., Hensel, V., Fanning, S., Schwarz, S., & Feßler, A. T. (2020). Biocide susceptibility testing of bacteria: Development of a broth microdilution method. *Veterinary Microbiology, 248*, 1087. https://doi.org/10.1016/j.vetmic.2020.108791

Shabaani, M., Rahaiee, S., Zare, M., & Jafari, S. M. (2020). Green synthesis of ZnO nanoparticles using loquat seed extract; biological functions and photocatalytic degradation properties. *LWT, 134*, 110133. https://doi.org/10.1016/j.lwt.2020.110133

Shaikh, A. F., Tamboli, M. S., Patil, R. H., Bhan, A., Ambekar, J. D., & Kale, B. B. (2019). Bioinspired carbon quantum dots: An antibiofilm agents. *Journal of Nanoscience and Nanotechnology, 19*, 2339–2345. https://doi.org/10.1166/jnn.2019.16537

Shameli, K., Ahmad, M. B., Zargar, M., Yunus, W. M. Z. W., Ibrahim, N. A., Shabanzadeh, P., & Moghaddam, M. G. (2011). Synthesis and characterization of silver/montmorillonite/chitosan bionanocomposites by chemical reduction method and their antibacterial activity. *International Journal of Nanomedicine, 6*, 271. https://doi.org/10.2147/IJN.S16043

Sivaramakrishnan, M., Sharavanan, V. J., Govindarajan, D. K., Meganathan, Y., Devaraj, B. S., Natesan, S., Kothandan, R., & Kandaswamy, K. (2019). Green synthesized silver nanoparticles using aqueous leaf extracts of *Leucas aspera* exhibits antimicrobial and catalytic dye degradation properties. *SN Applied Sciences, 1*, 28. https://doi.org/10.1007/s42452-019-0221-1

Soyuçok, A., Kart, A., Yalçın, H., Zeybek, E., & Özkan, O. (2023). Determination of in vitro antimicrobial and antibiofilm activity of Hypericum crenulatum against some food pathogens and its phenolic content. *Acta Alimentaria*. https://doi.org/10.1556/066.2023.00225

Soyuçok, A., Kiliç, G., Kiliç, B. (2019). Use of encapsulation technology in meat industry. The Journal of Graduate School of Natural and Applied Sciences of Mehmet Akif Ersoy University, 10 102–110. https://doi.org/10.29048/makufebed.530102

Sunil Kumar, M. S., Shubha, J. P., Nagaraju, G., Rekha, N. D., & Nirmala, B. (2022). Facile combustion derived synthesis of copper oxide nanoparticles: Application towards photocatalytic, electrochemical and DNA cleavage studies. *Nano-Structures & Nano-Objects, 32*, 100923. https://doi.org/10.1016/j.nanoso.2022.100923

Tel-Çayan, G., Duru, M. E. (2019). Chemical characterization and antioxidant activity of Eryngium pseudothoriifolium and *E. thorifolium* essential oils. *Journal of Research in Pharmacy*, 23(6) 1106–1114. https://doi.org/10.35333/jrp.2019.75

Thiviya, P., Gamage, A., Piumali, D., Merah, O., & Madhujith, T. (2021). Apiaceae as an important source of antioxidants and their applications. *Cosmetics, 8*(4), 111. https://doi.org/10.3390/cosmetics8040111

Thiviya, P., Gunawardena, N., Gamage, A., Madhujith, T., & Merah, O. (2022). Apiaceae family as a valuable source of biocidal components and their potential uses in agriculture. *Horticulturae, 8*(7), 614. https://doi.org/10.3390/horticulturae8070614

Trak, D., Arslan, Y. (2021). Synthesis of silver nanoparticles using dried black mulberry (*Morus nigra L.*) fruit extract and their antibacterial and effective dye degradation activities. *Inorganic and Nano-Metal Chemistry*, 1–13. https://doi.org/10.1080/24701556.2021.1980038

Trak, D., & Arslan, Y. (2022). Biosynthesis of gold nanoparticles (AuNPs) with Dimrit raisin extract and their degradation activity for water contaminants. *Duzce University Journal of Science and Technology*, 10, 117–127. https://doi.org/10.29130/dubited.901949

Tripathi, R. M., Hameed, P., Rao, R. P., Shrivastava, N., Mittal, J., & Mohapatra, S. (2020). Biosynthesis of highly stable fluorescent selenium nanoparticles and the evaluation of their photocatalytic degradation of dye. *BioNanoScience, 10*, 389–396. https://doi.org/10.1007/s12668-020-00718-0

Veza, I., Spraggon, M., Fattah, I. R., Idris, M. (2023). Response surface methodology (RSM) for optimizing engine performance and emissions fueled with biofuel: Review of RSM for sustainability energy transition. *Results in Engineering*, 101213. https://doi.org/10.1016/j.rineng.2023.101213

Wang, H., Al-Kurdhani, J. M. H., & Ma, J. (2023). Wang, Adsorption of Zn^{2+} ion by macadamia nut shell biochar modified with carboxymethyl chitosan and potassium ferrate. *Journal of Environmental Chemical Engineering, 11*, 110150. https://doi.org/10.1016/j.jece.2023.110150

Zhang, Z., Li, S., Gu, X., Li, J., Lin, X. (2019). Biosynthesis, characterization and antibacterial activity of silver nanoparticles by the Arctic antioxidative bacterium *Paracoccus* sp. Arc7-R13. *Artificial Cells, Nanomedicine, and Biotechnology,* 47(1), 1488–1495. https://doi.org/10.1080/21691401.2019.1601631

Zhou, Y., Kong, Y., Kundu, S., Cirillo, J. D., & Liang, H. (2012). Antibacterial activities of gold and silver nanoparticles against *Escherichia coli* and *bacillus* Calmette-Guérin. *Journal of Nanobiotechnology, 10*, 1–9. https://doi.org/10.1186/1477-3155-10-19